Expansion of Emmental cheese and tofu using instant controlled pressure drop (DIC) process

Ismail Sulaiman, Lukáš Krátký, Karim Allaf, Václav Sobolík, Magdalena Kristiawan

Expansion of Emmental Cheese and Tofu using Instant Controlled Pressure Drop (DIC) Process

Ismail Sulaiman[1], Lukáš Krátký[2], Karim Allaf[3], Václav Sobolík[3], Magdalena Kristiawan[4,*]

[1] Department of Agricultural Product Technology, Faculty of Agriculture, Universitas Syiah Kuala, Indonesia.
[2] Czech Technical University, Faculty of Mechanical Engineering, Department of Process Engineering, Technická 4, 160 00 Prague 6, Czech Republic.
[3] LaSIE, UMR 7356, University of La Rochelle, 17 062 La Rochelle, France.
[4] INRAE UR 1268, Biopolymers, Interactions & Assemblies (BIA), 44316 Nantes, France,
*corresponding author: magdalena.kristiawan@inrae.fr.

Abstract

Two foods, belonging to different protein sources (dairy vs plant), namely Emmental cheese and tofu, were treated by the instant pressure drop (DIC) process inserted between two drying stages to obtain expanded and crispy snacks. This process consisted of a short heating step (t = 38 – 52 s) using steam under pressure (p = 0.26 – 0.62 MPa) and instantaneous pressure drop toward a vacuum. This pressure drop provoked auto-vaporization of the superheated liquid, which resulted in volume expansion, and cooling of the food. The expansion was visualized using a rapid camera at a frequency of 1000 images/s. The pressure and temperature histories were registered simultaneously. Three expansion ratios were evaluated: i) r the ratio of food volumes after and before DIC process measured using sand pycnometry, ii) r_C calculated from dimensions measured by a caliper, and iii) r_I calculated from dimension reading from images. The shrinkage $s = (r_I / r_C) - 1$, and the deformation $d = (r_C / r) - 1$ of the samples were then evaluated. Using response surface methodology, the optimal processing conditions for maximum expansions r = 2.5 and r_C = 4.5 were found for Emmental and tofu, respectively as p = 0.5 and 0.62 MPa, t = 40 and 38 s. The creation of mist, inherent to the pressure drop of steam, made the visual observation impossible at the beginning of pressure drop. The samples were already expanded when the mist disappeared. Taking the mist presence as the upper limit of expansion time, the expansion took dozens of milliseconds at a pressure drop rate of 1.25 MPa/s. The temperature in the reactor decreased at a rate of 750 °C/s.

Keywords: food expansion, Instant Controlled Pressure-Drop DIC, drying, response surface methodology, rapid camera.

1. Introduction

Instant Controlled Pressure Drop DIC process is a pioneering technology used for the transformation of raw foods to ready-to-eat products by changing their structure and texture (Allaf et al., 1995). The DIC process resembles to puffing (Schwartzberg et al., 1995; Singh and Singh, 1999) or extrusion cooking (Moraru and Kokini, 2003; Arhaliass et al., 2009), but the DIC exhibits are three essential differences, (a) pressure drop from high pressure towards vacuum, (b) process rapidity, and (c) possible applications to materials with a low glass

transition temperature. This results in important modification and preserving effects on structural, textural, and sensorial properties and nutritional and microbiological quality of products thanks to the exposition to high temperature for a very short time.

The DIC process was originally used as pre-treatment stage for drying of fruits and vegetables (Louka and Allaf, 2004; Albitar et al., 2011). Partially dehydrated products were heated in an autoclave using steam for dozens of seconds and then the pressure was rapidly decreased to vacuum. The explosively evaporated superheated moisture inside the products created a porous structure. The moisture content did not change much during this process but the structure was expanded with open pores, which accelerated the final drying in a classical oven. Besides the drying, the DIC process was used for the extraction of essential oils (Kristiawan et al., 2008). To reach a high yield, the heating and pressure drop steps were repeated several times. Similar idea was applied in multi-flash process for producing dehydrated crispy fruits (Zotarelli et al., 2012). The fruits were heated by hot air under ambient pressure and a vacuum pulse was repeatedly applied.

State diagram for starchy food expansion by DIC can be adopted from the pathway of starchy foods expansion during extrusion (Van der Sman and Broeze, 2014; Kristiawan et al., 2016) as follows. Upon heating during saturated steam injection in the autoclave, the food matrix is humidified and molten. When abrupt pressure drop into vacuum take place, moisture flushes off and the expansion occurs instantaneously. The rapid decline in product temperature and moisture content is accompanied by a rapid increase in glass transition temperature (Tg), as bubbles undergo rapid expansion. The bubbles expand if melt temperature is higher than 100 °C. Depending on initial moisture conditions, the bubble can experience shrinkage as the melt temperature decreases below 100 °C due to vapor condensation. During cooling, when atmospheric pressure is re-installed, the product temperature becomes lower than Tg, and the structure sets to glassy state. This texturing depends not only on the composition of the food under consideration, but also on the treatment conditions, over-heating levels and evolution of rheological properties of the food generated by biopolymers changes. All these variables are highly interdependent. The changes of biopolymers range from starch melting and depolymerization (Logié et al., 2018), protein denaturation and aggregation (Stanley, 1989), fiber solubilization to lipid expulsion (Ralet et al., 1993; Everett and Auty, 2008). Besides the effect on rheological properties (melt viscoelasticity, stretchability and elongation), the constituents (starch, protein), even minor ones (fat/oil, fiber), affect also glass transition temperature. Both variables, melt rheology and Tg, are considered as key factors in expansion (Della Valle et al., 1997). Starch is a role component in the production of expanded snacks because its content and amylose/amylopectine proportion control melt rheology. For example, Chanvrier et al. (2015) found that molten maize flour and molten starch-zein mixture (85% - 15%) have a shear viscosity very close to that of maize starch. Concerning cheese, having fat as major component (around 50% of dry matter), our first trial have proved that DIC leads to expulsion of a significant amount of fat. Modification of fat content can alter the melt rheology and in-turn the expansion level of cheese.

Aerated foods, including snacks and breakfast cereals, constitute one of the fastest growing food sectors. Most of these foods, rich in starch and processed by extrusion, have major drawbacks: they are rapidly digested and have a high glycemic index (GI) due to their high sugar content and highly destructured state of starch owing to extrusion. These high GI foods are consumed primarily by children and young adults. It is one of the factors favoring the increase of obesity of this population. While starch-based aerated foods fill supermarkets (e.g. the breakfast cereal and aperitifs aisles), the protein-rich alternatives are quite rare. Protein-rich aerated foods, mostly based on plants, are not equally appealing to consumers in terms of their textural and sensorial properties, because very little is known about the dynamics of bubbles formation in protein-rich food-matrices during processing.

The DIC swell-drying is able to texturize thermo-labile food ingredients, to obtain final products with remarkable properties: expanded structure (crispy), grinding ease, fast rehydration kinetics, good nutritional characteristics and high organoleptic quality (Allaf and Allaf, 2014). Emmental cheese, highly appreciable by western society, has incredible, taste in its natural state, and it provides health benefits if consumed moderately. Some authors have shown that imitation/reconstituted cheese (having major constituents of rennet casein, emulsifying salts, and resistant starch) can be transformed into healthy crispy snacks using microwave expansion (Arimi et al., 2010).

Tofu (soy curd), made from coagulated and pressed soy milk, is a widely consumed food by Asian population due to its rich nutritional value and health benefits to the human body (Xu et al., 2016). Due to limitations linked to stability of fresh tofu, providing a dried form of tofu, having better nutritional value than conventional one, can increase benefit of this traditional food, labelled since longtime as staple food for poor people. In Chinese culinary tradition, dried tofu can be either processed further to make other recipes: fermented tofu, smoked tofu, five-spice tofu, or be utilized as an ingredient protein source in instant soups/noodles.

In this paper, we studied the effect of DIC parameters on the expansion characteristics of protein-based snacks. Two food models representing dairy and vegetal protein sources were chosen: emmental cheese and tofu. The highly expanded structure of DIC treated products is very important, because the ultimate goal is to produce a crunchy/crispy and tasty post-dried snacks. Structural features, such as expansion ratio, shrinkage and deformation attributes were determined. Experimental design and statistical analysis were employed to determine DIC parameters leading to optimum expansion characteristics. For the first time, dynamics of expansion during pressure drop was studied using a high-speed camera (1000 frames/s) and image analysis. The pressure and temperature history of product and steam inside the autoclave were registered simultaneously with the camera frames. Using these data, new insight into the expansion phenomena was discussed.

2. Experimental

2.1. DIC setup

The schema of DIC setup is shown in Fig. 1a and a photography in Fig. 1b. It consisted of an 18 L autoclave (1) with an inspection window, a 1600 L vacuum tank (2), a water ring

vacuum pump (3) and a trap (4). The autoclave communicated with the reservoir using a pneumatically driven butterfly valve (V2) in a stainless steel tube with a diameter of 180 mm and a length of 0.8 m in the form of a 90° elbow. The saturated steam S1 (700 kPa/165 °C) was fed into the autoclave through a valve V1. The pressure and heating time in the autoclave was controlled manually by opening and closing this valve in function of the pressure red on the gauge P and a stopwatch. The decompression (pressure drop rate) in the autoclave was given by the opening rate of the pneumatically driven valve V2. This rate was not controlled. Ambient pressure was installed in the autoclave using a vent (V3). The double jacket of the autoclave was heated by steam S2.The vacuum tank (2) was cooled by tap water (W1) circulating in a double jacket.

Food samples were put into and discharge manually from the autoclave through a cover with bayonet joint. In the open position, the cover was heated using a 1000 W infrared quartz radiator to decrease condensation inside the autoclave during sample treatment.

The autoclave was equipped with the pressure gauge P, thermometer T, pressure sensor Baumer PBSN 0 -1 MPa with a rise time (10 ... 90 %) ≤ 5 ms, and thermocouples type K (conductor diameter 0.3 mm with an exposed measuring junction) for measuring the temperatures inside the autoclave and in sample. The sensors were connected to signal conditioners Loreme Cal 30. There was no back-feed from sensors to valves. The valves were actioned either manually (V1, V3-V7) or pneumatically through an electrical relay (V2).

The evolution of sample expansion in the autoclave during pressure drop was captured *in situ* using a high-speed camera through a glass inspection window with a diameter of 100 mm. There were six halogen bulb H1 (6x100 W) in front of the window to ensure the product illumination and to heat the window to eliminate steam condensation. The camera and illuminated window are in the front of photography (Fig. 1b). The six white cables supply the bulbs. The autoclave (1) is insulated by aluminum sheet. The butterfly valve (V2) is below and the vacuum tank (2) is rear the autoclave. The electrical board is on the right.

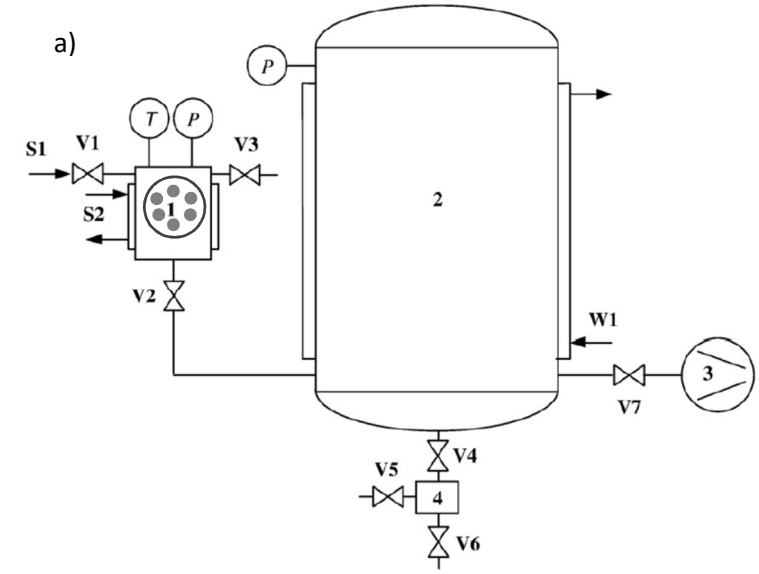

Fig. 1a. Schema of DIC setup. 1 – autoclave with inspection window and bulbs, 2 – vacuum tank, 3 – vacuum pump, 4 – trap for condensate.
1b. Photography of DIC equipment. The rapid camera and illuminated window are in the front of the insulated autoclave. The vacuum tank is behind and the valve V2 bellow the autoclave.

2.2. DIC treatment

Food sample was pushed on a stainless steel wire with a diameter of 2 mm supported by a U-shaped stainless steel holder and placed into the autoclave. The autoclave cover was closed (stage a in Fig. 2) and the valve V2 was opened to install vacuum in the autoclave (stage b). In this way, the quantity of gas in the sample was lowered to facilitate steam penetration in the next stage. The valves V2 was closed and V1 opened (stage c). The time of exposure to steam (stage d) was measured from the moment when the pressure reached the prescribed value. As condensation took place in the autoclave, it was necessary to control the pressure manually using the valve V1 (stage d). When the time of exposure elapsed, the valve V1 was closed and V2 opened. The pressure dropped rapidly to a vacuum level (stage e). This abrupt adiabatic pressure drop resulted in vaporization of superheated liquid in the sample, which led to its swelling and instantaneous cooling. The vacuum was kept for a short time (stage f). Finally, the atmospheric pressure was restored in the autoclave by the vent (V3) and the sample was recovered (stage g). The pressure in the reservoir (2) was almost constant and equal to 10 kPa. The time t and pressure p of the stage d were controlled processing parameters.

2.3. Image and data acquisition

The evolution of product expansion during pressure drop was filmed using a rapid camera Photron Fastcam 1024 PCI with a resolution of 1024 x 1024 pixels with an 8-bit grayscale. The installed memory of 8 GB allowed us to take a record of 6.4 s at a frequency of 1000 frame/s. The camera was equipped with an objective Nikon 24 – 70 mm, F 2.8. This camera was also used to film the whole DIC process at a slow frequency of 30 frame/s.

The course of temperature and pressure inside the autoclave and temperature of sample during the pressure drop were registered at a frequency 1250 s^{-1} using a CONTEC AD12-16U (PCI) EV card. This card was triggered simultaneously with the Photron camera.

LabView virtual instrument with a card PCL 812 was used for acquisition of temperature and pressure at a frequency of 10 s^{-1} in the whole course of DIC process, see Fig.2.

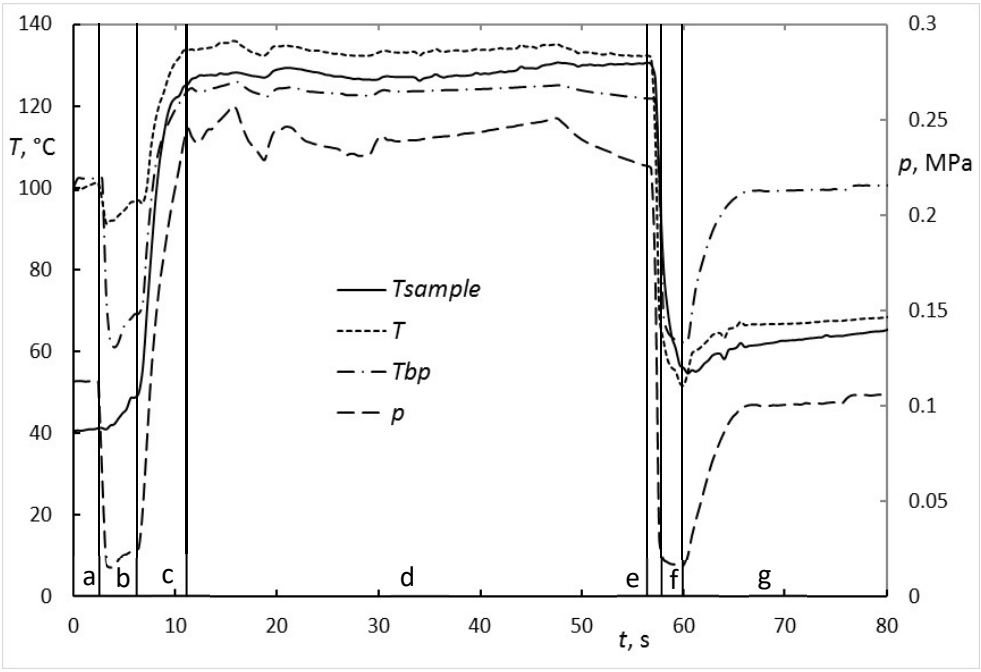

Fig. 2. Pressure and temperature histories of DIC process (Emmental cheese, 0.26 MPa, 45s). *Tsample* – temperature inside product, *T* – temperature of steam in autoclave, *Tbp* – saturated steam temperature corresponding to pressure, *p* – pressure of steam in autoclave.

2.4. Material

The effect of DIC parameters on the expansion characteristics of protein based foods was studied using two representatives of dairy and vegetal protein sources such as French Emmental cheese Entre Mont, and traditional tofu (soybean curd). The composition of these foods in raw state and after pre-drying before DIC treatment is given in Table 1. The initial size and moisture content of samples have a great effect on the treatment. In this study, these two parameters were kept constant. Emmental cheese was cut to pieces of 20 x 15 x 15 mm^3 and pre-dried in a force convection oven (Memmert 800) at 37°C during 12 hours to a moisture content of 10 % dry matter basis (d.m.). Tofu was cut to pieces of 14 x 15 x 10 mm^3 and dried in the Memmert oven at 37° to a moisture content of 17 % d.m.

Table 1. Composition of Emmental cheese and tofu in raw and pre-dried states before DIC treatment.

	Emmental cheese		Tofu	
	raw	pre-dried	raw	pre-dried
	g / 100 g	% of dm	g / 100 g	% of dm
Eau	44.9	10	84.9	17.0
protein	26	47.2	8.2	54.3
lipide	28	50.8	4.2	27.8
glucide	0.5	0.9	1.7	11.3
fibres	0	0.0	1	6.6
sel	0.6	1.1	0	0.0

The moisture content of foods changes during DIC treatment depending on injected steam pressure. As it is not feasible to measure moisture content in real-time, only the moisture

content of final post-dried samples was determined. Emmental cheese and tofu was post-dried in the Memmert oven to a final moisture content of 7% d.m. and 10% d.m., respectively.

2.5. Methods of analyses

The structural features of expanded foods were determined quantitatively in the following manner. The true expansion ratio (r) was defined as the volume of a sample after DIC treatment and post-drying (V_{DIC}) divided the volume of sample before DIC treatment (V_R)

$$r = \frac{V_{DIC}}{V_R} \quad (1)$$

Volumes were obtained by a sand pycnometry method using fine sand (400 μm) and a graduated cylinder. Sample of known weight m_P and sand of specific mass ρ_S (1700 kg/m^3) were put into the cylinder, tapped and the whole volume V_W and mass m_W were measured. The volume of product V_P was calculated as

$$V_P = V_w - \frac{m_W - m_P}{\rho_S} \ . \quad (2)$$

Besides this true expansion ratio, two other ratios were evaluated. The ratio r_C was obtained from samples at the same state as in the case r, but the volumes $V_{DIC,C}$ and $V_{R,C}$ were approximated by rectangular parallelepipeds of dimensions measured using a caliper,

$$r_C = \frac{V_{DIC,C}}{V_{R,C}} \ . \quad (3)$$

As the samples were not always exact rectangular parallelepiped with planar sides, this ratio was different from the true ratio which follows all the form irregularities. This difference was expressed using the deformation index d,

$$d = (r_C / r) - 1. \quad (4)$$

The third ratio r_I is based the sample volumes immediately before and after pressure drop. These volumes, $V_{R,I}$ and $V_{DIC,I}$, were calculated from the dimensions revealed from 2D images recorded by the rapid camera (1000 frame/s during 6.4 s) before and after pressure drop, respectively. The third dimension necessary for the calculation of rectangular parallelepiped volume, the depth, was calculated as the arithmetic mean of the front dimensions,

$$r_I = \frac{V_{DIC,I}}{V_{R,I}} \ . \quad (5)$$

The main difference between this ratio and the r_C ratio was caused by the shrinkage of the samples after leaving the autoclave and due to the post drying. The shrinkage index was calculated as

$$s = (r_I / r_C) - 1 \quad (6)$$

Optimization of expanded food should be based on the compromise between volume expansion and deformation.

The glass transition temperature *T*g was determined by differential scanning calorimetry (DSC) using a T.A. Q100 instrument (TA Instruments, New Castle, Delaware, USA). The system was calibrated with indium. Measurements were carried out with 10 mg samples sealed in aluminum cells, to prevent loss of water during analysis. Two successive scans were run at 3°C/min between 10 and 120 °C (or 150°C for moisture content less than 11% w.b.), separated by a cooling stage, to eliminate any thermal event due to the aging during storage. The glass transition temperature was determined at the midpoint of the calorific capacity change during the second scan.

2.6. Experimental design

Similar to DIC treatment of any product (Louka and Allaf, 2004), the structure of the expanded cheese and tofu mainly depends on the operating conditions such as steam pressure that defines the temperature, processing time and initial humidity of the food in question.

The DIC treatment was applied with the aim to obtain highly expanded and porous structure of Emmental cheese and tofu. Generally, the higher the expansion the crispier are the pieces of post-dried foods (Agbisit et al., 2007). The experimental design was used to find a set of DIC parameters (pressure and time of stage *d*, Fig. 2), which results in maximum of expansion ratios (r - Eq.1, r_I - Eq.5 and r_C - Eq.3), and low deformation (d - Eq.4) and shrinkage (s - Eq.6) of products. Preliminary experiments were carried out to estimate moisture content and the intervals of pressure and time in which the maximum of expansion lies. The optimum moisture content was found as 10 % and 17 % d.m. for Emmental chesse and tofu, respectively. The steam pressure p lay in an interval 0.3 to 0.5 MPa for Emmental cheese and 0.5 to 0.6 MPa for tofu while the range of the thermal treatment duration t was from 40 to 50 s for both materials.

Response surface methodology tool of Statgraphics Centurion 18 software (Statgraphics Technologies, Inc.) was used for building experimental design and data treatment. Full central composite design with two factors (p, t) and five replicates at the central point, i.e. a total of 13 experiments was employed to evaluate the effect of DIC treatment on the structural features (r, r_C, r_I, s, d) and duration of mist in the autoclave (t_M). The mist formation is inherent effect of vapor condensation due to the pressure drop. The values of p, t factors for 13 experiments are given in Tables 2 and 3.

Table 2. Experimental design and results of expansion for Emmental cheese. Pressure p and time t of the DIC treatment (phase d in Fig.2), expansion ratios r (Eq.1), r_C (Eq.3) and r_I (Eq.5), shrinkage s (Eq.6), deformation d (Eq.4) and duration of mist t_M.

N° exp	p, MPa	t, s	r	r_C	r_I	s	d	t_M, ms
1	0.40	45.0	2.72	2.71	5.45	1.01	0.00	171
2	0.40	52.1	2.05	3.3	6.31	0.91	0.61	137
3	0.40	45.0	2.43	2.85	5.35	0.88	0.17	156
4	0.30	50.0	1.99	2.68	4.41	0.65	0.35	125
5	0.50	40.0	2.78	3.24	5.51	0.70	0.17	144
6	0.40	45.0	2.53	2.79	5.21	0.87	0.10	133
7	0.40	45.0	2.43	2.71	5.41	1.00	0.12	138
8	0.40	37.9	1.82	2.06	4.26	1.07	0.13	160
9	0.30	40.0	1.5	1.8	3.77	1.10	0.20	-
10	0.26	45.0	2.01	2.17	2.94	0.35	0.08	68
11	0.40	45.0	2.11	2.82	5.29	0.87	0.34	153
12	0.50	50.0	1.58	2.54	3.85	0.51	0.61	143
13	0.54	45.0	1.88	2.71	6.66	1.46	0.44	139

Table 3. Experimental design and results of expansion for tofu. Pressure p and time t of the DIC treatment (phase d in Fig.2), expansion ratios r_C (Eq.3) and r_I (Eq.5), shrinkage s (Eq.6), and duration of mist t_M.

N° exp	p, MPa	t, s	r_C	r_I	s	t_M, ms
1	0.55	45	3.59	6.47	0.80	143
2	0.55	52	3.72	6.41	0.72	167
3	0.55	45	3.36	7.52	1.24	169
4	0.60	40	3.15	8.37	1.66	159
5	0.55	38	2.79	6.68	1.39	133
6	0.48	45	2.53	5.33	1.10	101
7	0.55	45	2.94	9.00	2.06	141
8	0.55	45	3.10	6.57	1.12	136
9	0.62	45	4.45	9.50	1.14	131
10	0.55	45	3.04	6.59	1.17	186
11	0.50	40	2.32	4.96	1.14	186
12	0.60	50	2.34	6.85	1.93	111
13	0.50	50	3.08	7.75	1.52	80

3. Results and discussion

3.1. Visual observation

3.1.1 Emmental images

The Fastcam registered 6400 shots at a frequency of 1000 frame/s. The camera was started a few second before the pressure drop. The sequential shots showing characteristic moments of Emmental cheese during pressure drop are shown in Fig. 3.

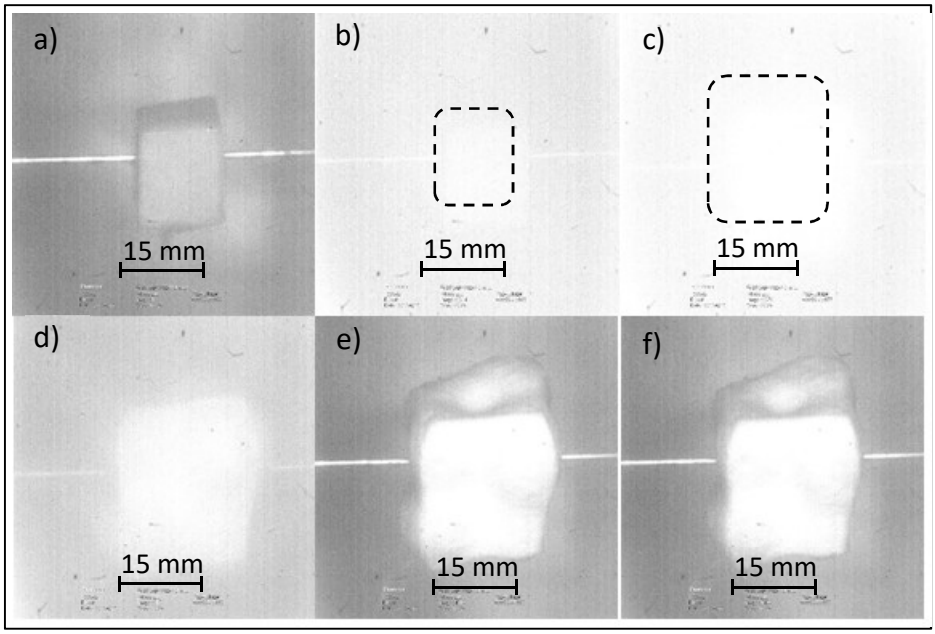

Fig. 3. Emmental cheese expansion from a pressure of 0.26 MPa after heating time of 45s. a) before pressure drop, current time t_C=1 ms; b) beginning of pressure drop, creation of mist, t_C= 3014 ms; c) sample emerging from mist, t_C = 3078 ms ; d) visible sample, t_C = 3133 ms; e) expanded sample, t_C = 4310 ms; f) expanded sample at the end of record, t_C = 6400 ms.

It was impossible to observe the sample through the mist created in the autoclave at the beginning of the pressure drop. When the mist disappeared, the sample was already expanded. Hence the period of sample expansion was less than or equal to the time of the mist presence, t_M. The time interval between the start of pressure drop accompanied by the mist creation (frame b) and the immerging of expanded Emmental cheese from the mist (frame c) was 64 ms. Hence the time of sample expansion was less or equal to 64 ms. The size of Emmental sample did not change during the short period after expansion (frames e and f). There is a view of Emmental cheese before and after DIC treatment in the direction of supporting wire in Fig.4.

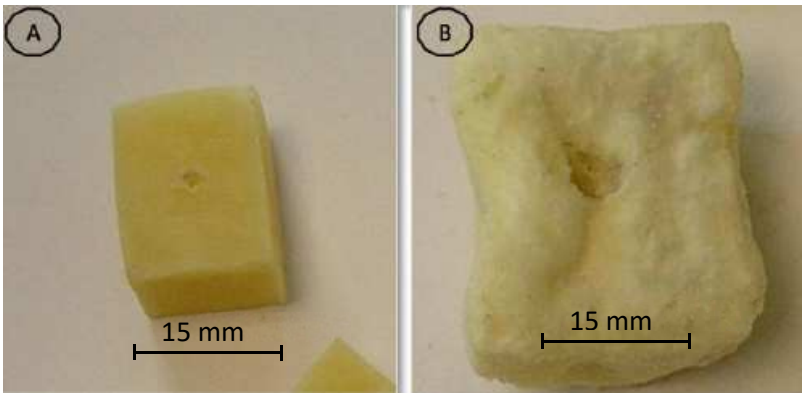

Fig.4. A) Emmental cheese before DIC treatment; B) expanded Emmental after treatment and post-drying.

The depth of the product is better visible in Fig.4 than in the images of rapid camera. The expansion of all three dimensions is similar, which validate the way of calculation r_I from 2D camera images.

The time of mist duration, t_M, is given in Table 2. This time increases slightly with the pressure and is invariant to the time of DIC treatment. An unknown quantity of condensed steam in the autoclave can be the most important factor of mist duration.

The whole DIC process, filmed by Photron Fastcam 1024 PCI camera at a frequency of 30 frame/s, is shown in Video 1. The following stages can be recognize in this film: installing the primary vacuum at 10 s (stage b in Fig. 2); opening the vapor valve V1 at 17 s (stage c); keeping the pressure and heating the product (stage d); pressure drop at 65 s (stage e) and keeping the vacuum (stage f). Droplets of fat and condensed water trickled from the Emmental cheese during the heating stage *d*.

3.1.2 Tofu images

Selected images of tofu treatment are shown in Fig. 5. The mist stayed for about 186 ms. Shrinkage of the sample was observed after expansion, compare the frames d, e and f.

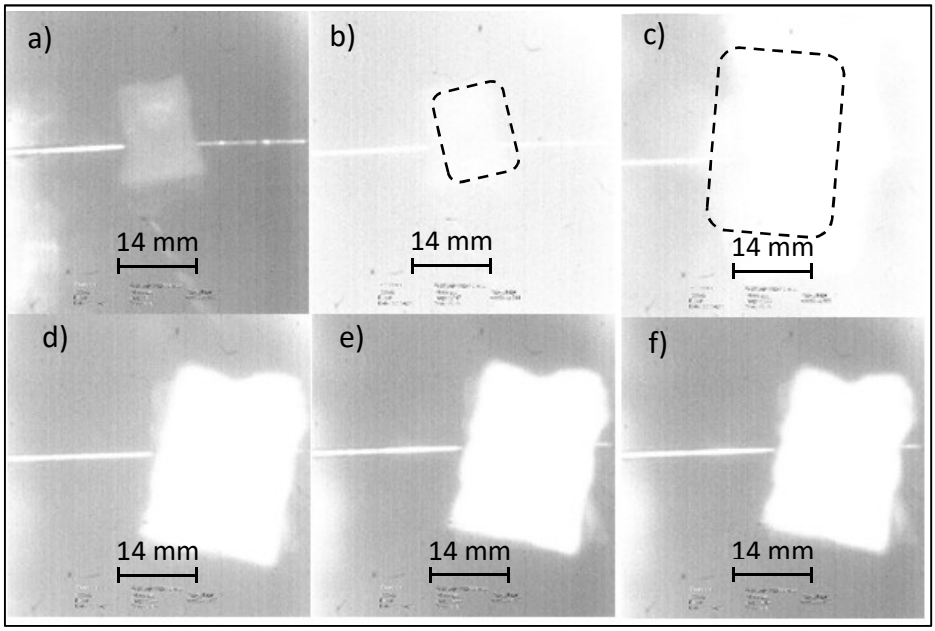

Fig. 5 Tofu expansion at a pressure of 0.55 MPa and heating time of 45s.
a) before detente, current time t_C =1 ms ; b) beginning of detente, creation of mist, t_C = 2745 ms ; c) sample emerging from the mist, t_C = 3000 ms ; d) visible sample, t_C = 3200 ms; e) expanded sample, t_C = 5000 ms; f) expanded sample at the end of record, t_C = 6400 ms.

3D view of tofu before and after DIC treatment is shown in Fig. 6. The expansion of tofu is more important than that of Emmental cheese.

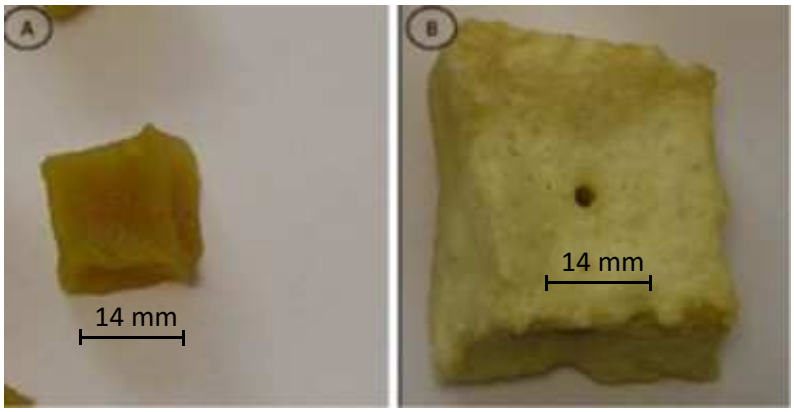

Fig.6. A) tofu before DIC treatment A; B) expanded tofu B.

3.2 Characteristics of expansion

3.2.1 Response surfaces of Emmental cheese

The expansion characteristics r, r_C, r_I, s and d, and the time of mist duration t_M are given in Table 2. Using the response surface methodology tool of software Statgraphics Centurion 18, the response surfaces were obtained as quadratic function of the steam pressure and heating time by means of variance analysis (ANOVA), see Fig. 7.
The response surface was described by the quadratic function of p and t

$$Response = a + b\,p + c\,t + d\,p^2 + f\,p\,t + g\,t^2 \quad . \qquad (7)$$

The coefficient for different responses are summarized in Table 4, together with optimum response values and factors, which were statistically significant at the 0.05 level. The optimum values for expansion r, r_I and r_C, and t_M are they maxima, while they are the minima for shrinkage s and deformation d.

Table 4. Coefficients of estimated response surfaces, Eq. 7, for Emmental cheese. The optimum responses of expansions r (Eq.1), r_I (Eq.5) and r_C (Eq.3), and duration of mist t_M are the maxima, while they are the minima for shrinkage s (Eq.6) and deformation d (Eq.4).

	Coefficients of response surface						Optimum			Significant
Response	a	b, MPa^{-1}	c, s^{-1}	d, MPa^{-2}	f, $(MPa\ s)^{-1}$	g, s^{-2}	Response	p, MPa	t, s	factors
r	-36.728	58.281	1.2250	-24.263	-0.845	-0.0099616	2.51	0.499	40.3	$p^2, p\,t, t^2$
r_I	-43.369	94.660	1.2052	-43.607	-1.15	-0.007758	6.03	0.541	37.9	p
r_C	-21.092	51.373	0.53294	-16.566	-0.79	-0.0018732	3.16	0.541	37.9	$p, t, p\,t$
s	1.1413	0.45591	-0.003612	-6.3541	0.13148	-0.000783	0.30	0.260	52.1	no
d	11.369	-10.499	-0.44540	6.1262	0.145	0.0046568	0.08	0.367	42.1	p, t, t^2
t_M*	-383.84	2326.0	1.8407	-2220.73	-8	0.0099591	161	0.455	37.9	p, p^2

* Units of t_M coefficients must be multiplied by second.

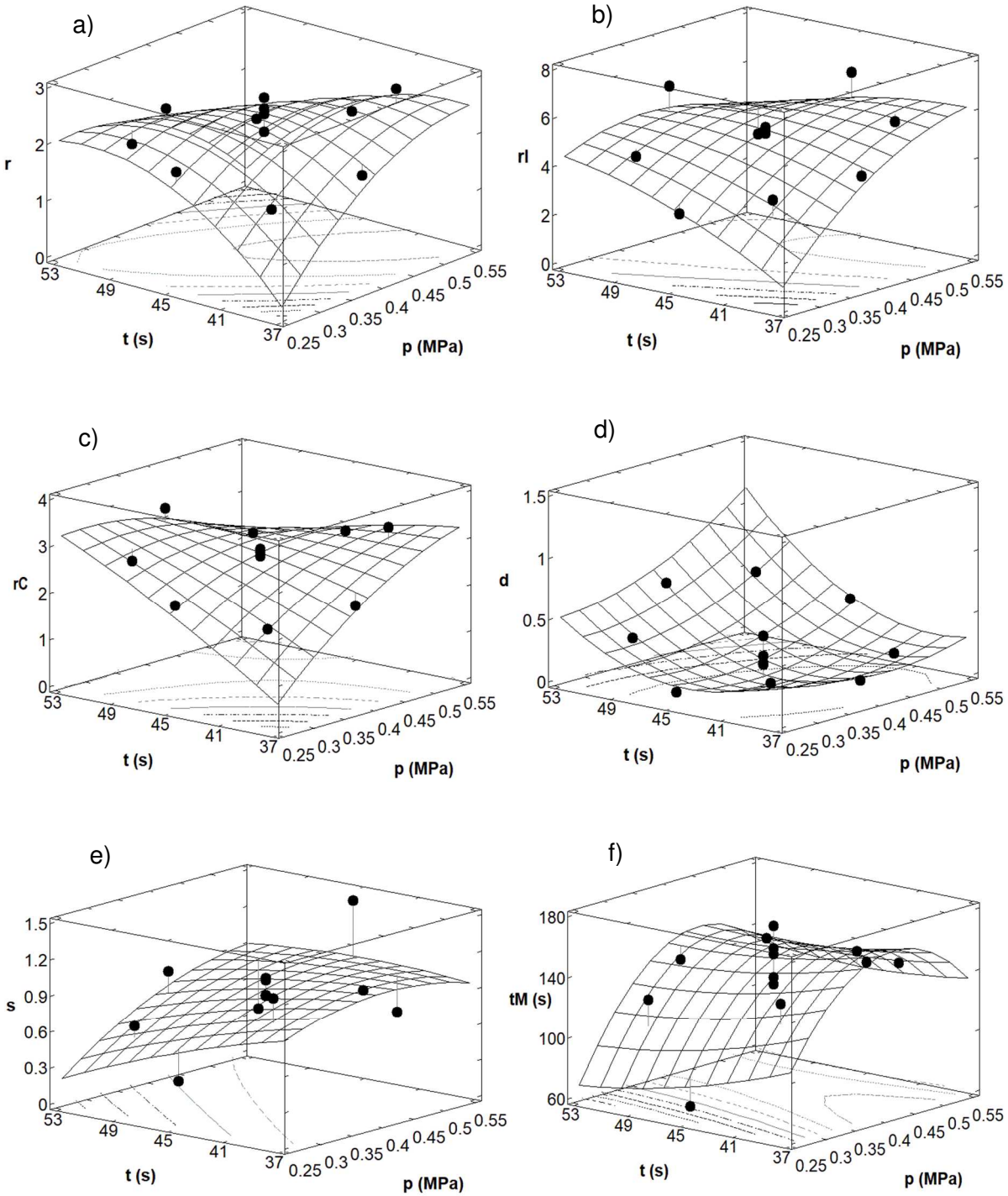

Fig. 7. Estimated response surfaces as function of pressure and heating time for Emmental cheese.
a) r – true expansion ratio (Eq.1); b) r_I – expansion ratio calculated from images immediately before and after pressure drop (Eq.5); c) r_C – expansion ratio calculated from dimensions measured by caliper (Eq.3); d) d – deformation (Eq.4); e) s – shrinkage (Eq.6); f) t_m – duration of mist.

The maximum value of the true expansion ratio, $r_{max,}$ is 2.5 at the factors p and t equal to 0.5 MPa and 40.3 s, resp (Fig. 7 and Table 4). The factors p^2, $p\ t$ and t^2 were statistically

significant at the 0.05 level (Table 4). At low pressure, the true expansion ratio r increased with increasing time while at high pressure the effect of time was opposite. For a short time, r increased with pressure and inverse at a long time. For high values of p and t, r was low due to high values of deformation and shrinkage. The Emmental cheese structure was not stiff enough to sustain contraction during and after the pressure drop. The shrinkage depends on the rheological properties and temperature during pressure drop. The studied foods (cheese and tofu) have a temperature and moisture content dependent shear-thinning behavior at molten state (Gunasekaran and Mehmet, 2002). The consistency decreases with increasing temperature, i.e. with increasing steam pressure. If the consistency is too low during and after expansion, the shrinkage of porous structure takes place.

The factors found for the $r_{I,max} = 6$, were a little different ($p_{opt} = 0.541$ MPa, $t_{opt} = 37.9$ s) from those for r_{max}. The factors for $r_{C,max} = 3.16$ are the same as the preceding ones. High values of expansion ratios lie on the diagonal low pressure – long time and high pressure – short time.

The samples were almost without deformation ($d = 0.08$) at $p = 0.367$ MPa and t=42.1 s. The true expansion ratio at these parameters ($r = 2.25$) was not far from its maximum. The shrinkage minimum ($s = 0.3$) was at low pressure (0.26 MPa) and long time (52.1 s) with corresponding $r = 2.12$. The maxima of s and d were about 1 but achieved at different factors. While the maximum s_{max} lay at the middle value of p interval (0.43 MPa) and minimum of t (38 s), the maximum of deformation occurred at maximum of p and t.
It is important for the aspect of a product that its deformation is not to large. The predicted deformation for r_{max} was rather low ($d = 0.184$).

3.2.2 Tofu

The response surfaces for tofu are shown in Fig. 8. The coefficient for different responses are summarized in Table 5, together with optimum response values and factors statistically significant at the 0.05 level.

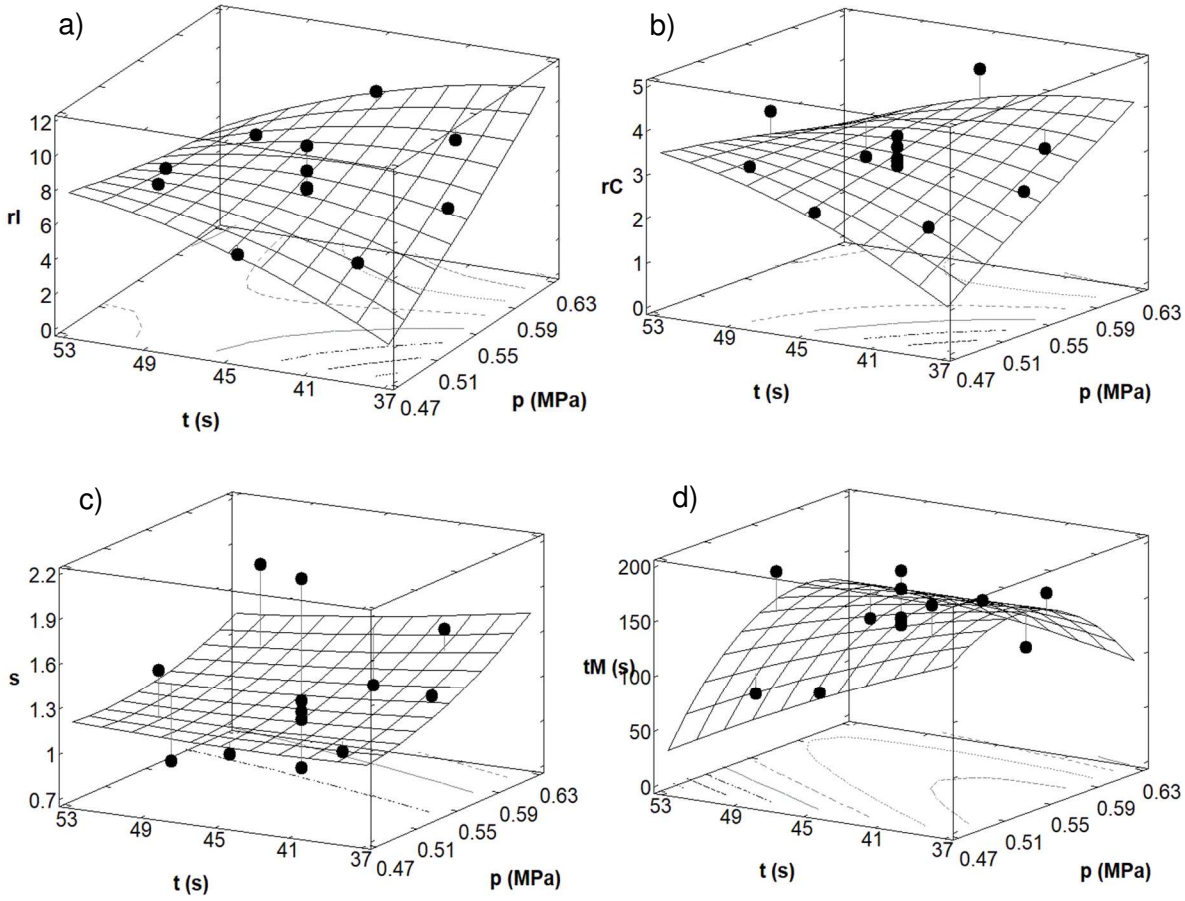

Fig. 8. Estimated response surfaces as function of pressure and heating time for tofu.
a) r_I – expansion ratio calculated from images immediately before and after pressure drop (Eq.5); b) r_C – expansion ratio calculated from mechanically measured dimensions (Eq.3) ; c) s – shrinkage (Eq.6); d) t_M – duration of mist.

The response surfaces of expansion rate calculated from images and caliper measurements were similar, see Figs 8 a, b, but the values of r_I were higher than that of r_C. The ANOVA analysis found $r_{I,max}$ = 10.2 and $r_{C,max}$ = 4.5 at p = 0.62 MPa and t = 37.9 s. For a low pressure, r_I, and r_C increased with the time of thermal processing, whereas the opposite trend was observed at a high pressure. The higher the pressure at short time, the higher were the expansion ratios. The almost planar response surface of shrinkage, Fig. 8c, predicted linear increase of s with pressure and independency on time. The shrinkage maximum corresponded to the maxima of expansion ratios.

The response surface of mist duration has similar form as in the case of Emmental cheese. It is not surprising, as small samples did not affect thermodynamic of gas in the autoclave. The predicted time of mist was between 100 and 172 s.

The expansion ratios of tofu were greater than that of Emmental chesse, but they were still much smaller than that for Emmental cheese powder published by Mounir et al. (2011), who found as high values as 36.

Table 5. Coefficients of estimated response surfaces, Eq. 7, for tofu. The optimum responses of expansions r_I (Eq.5) and r_C (Eq.3), and duration of mist t_M are the maxima, while it is the minimum for shrinkage s (Eq.6).

	Coefficients of response surface						Optimum			Significant
Response	a	b, MPa^{-1}	c, s^{-1}	d, MPa^{-2}	f, $(MPa\ s)^{-1}$	g, s^{-2}	Response	*p*, MPa	*t*, s	factors
r_I	-128.64	174.31	3.6289	36.994	-4.31	-0.013736	10.18	0.62	37.9	*p*
r_C	-60.493	73.168	1.8347	24.402	-2.04	-0.007918	4.47	0.62	37.9	*p*, *p t*
s	2.9346	-10.081	0.026846	16.078	-0.11383	0.0003128	1.19	0.497	47.2	no
t_M*	-886.39	6025.7	-26.109	-7746.4	58	-0.09388	171.9	0.531	37.9	no

* Units of t_M coefficients must be multiplied by second.

3.3. Pressure drop and temperature of glass transition

The history of the pressure and temperatures during the pressure drop is shown in Fig. 9. The first vertical dotted line stands for the start of pressure drop accompanied with creation of mist. The creation of mist is an inherent process during adiabatic steam expansion. The second line represents the mist disparition after 68 ms. At this moment, the Emmental cheese was already expanded. The pressure stood constant or even raised for a short time immediately after mist disparition. This effect was observed in all experiments. The pressure decreased rapidly, at an initial rate of 1.25 MPa/s. Details about the calculation of initial pressure drop rate can be found in Kristiawan et al. (2008b). About 300 ms were necessary to install vacuum. The temperature in the reactor (T reactor) at a rate of 750°C/s. Due to the adiabatic expansion, this temperature fell below the equilibrium temperature corresponding to the saturated steam pressure (Tbp) at a time of 0.2 s. After 260 ms, the both temperatures aligned. The thermocouple placed inside the Emmental cheese showed a gradual decrease of sample temperature (T product). The sample cooled down to 80°C in about 1 s. The shrinkage of the sample took place at temperature above 100°C. The structure was set up in about 0.4 s after the start of pressure drop.

The temperature in the reactor during the heating stage (d in Fig.2) was superior to the equilibrium temperature of saturated steam. Due to throttling in the entry valve (V1 in Fig.1) the steam S1 became overheated. The initial pressure drop rate depended on the pressure *p*. The higher the pressure the faster was the decompression.

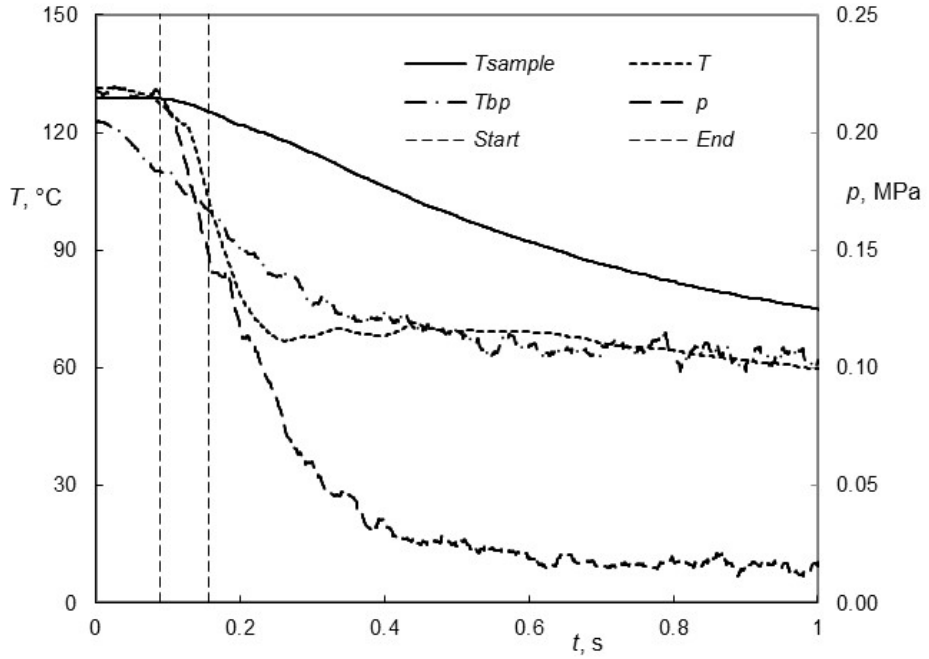

Fig. 9. Temperature and pressure history during detente of Emmental cheese (0.26 MPa and 45s). Zoom of stages e and f in Fig.2. *Tsample* – temperature inside product, *T* – temperature of steam in autoclave, *Tbp* – saturated steam temperature corresponding to pressure, *p* – pressure of steam in autoclave.
Start of pressure drop and creation of mist, *End* (disparition) of mist.

The DIC treatment reduced the temperature of glass transition of both foods. Original T_g of 37.0°C and 38.1°C decreased to 34.2 ± 1.2 °C and 35 ± 2.8 °C of Emmental cheese and tofu, respectively. Bubble expansion stops when product temperature crosses glass transition temperature (Tg) and therefore the structure is set. The higher Tg, the sooner the structure setting and the higher its expansion characteristics. The higher Tg of tofu can explain its higher expansion ratio than that of Emmental cheese.

4. Discussion

In analogy with mechanism of starchy melts expansion by extrusion (Kristiawan et al., 2016), the expansion using pressure drop in DIC treatment is controlled by several mechanisms: bubble nucleation, bubble growth, bubble coalescence, shrinkage, collapse, and texture setting. Nucleation and bubble growth have positive effect on expansion while coalescence and shrinkage exhibit negative effect. The expansion has optimum once the setting starts at the state of maximum bubble growth. Even if the values of parameters are different for DIC and extrusion processes, the expansion mechanisms are the same. The pressure, temperature, time, formulation (constituents), and melt physical properties (rheology, glass transition temperature), as a result of interaction among these factors, play key roles in product expansion.

In general, at the stage d in Fig. 1, the increase of temperature and exposition time can favor protein cross-linking and intermolecular reactions between protein and carbohydrates / starch and as a result, the melt viscosity increases (Verbeek and van den Berg, 2010). The

processing temperature of tofu, expressed by saturated steam pressure, was higher than that of Emmental cheese. The carbohydrate content of tofu was 12 times higher than Emmental cheese (11.3 % d.b. vs 0.9% d.b). The protein content of both foods did not differ much: 54.3% d.b. (tofu) vs 47.2% d.b. (Emmental cheese). The remnant of oil / fat, present in a higher amount in cheese than tofu, can act as internal lubricant.

The temperature and fat can be viscosity depressor while the carbohydrates/starch and protein aggregates can produce contradictory effect on viscosity. To favor expansion, melt viscosity should be low enough to promote the bubble growth but high enough to prevent bubble collapse and coalescence and hence product shrinkage (Kristiawan et al., 2016). The glass transition temperature of tofu was higher than that of Emmental cheese. High glass transition temperature can promote expansion by limiting collapse and shrinkage through earlier product structure setting. A longer contact time between food and steam can result in increased moisture content. The negative effect of moisture content on expansion can be linked to its depressor action on the viscosity, that controls bubble growth (Amon and Denson, 1984), and to reduction of glass transition temperature that controls the product setting (Della Valle et al. 1997). Therefore, the optimum melt viscosity and glass transition temperature should be set through optimum temperature (pressure in DIC process) and heating time to obtain maximum expansion. As the expansion ratio of tofu was higher than that of Emmental cheese, the melt viscosity of tofu was probably closer to its optimal value.

A special attention should be focused on the third ingredient (fiber) that makes up 6.6% of tofu components but being absent in Emmental cheese. Fiber can be considered as a filler in the continuous melt matrix. Fillers often enhance nucleation, allow cell opening, and modify rheological properties by reinforcing cell walls (Van der Sman, 2016, Kristiawan et al., 2016). Therefore, their presence favors expansion. On the other hand, fiber can decrease glass transition temperature and thus promote bubbles shrinkage and collapse. Fiber decreases melt elasticity and elongational viscosity (Robin et al., 2011, Robin et al., 2012) so bubble growth is hindered and bubble coalescence is favored. Poor physicochemical compatibility between the fiber particles and continuous phase can cause a low interfacial adhesion, leading to bubble ruptures (Robin et al. 2012 b). Fiber action on structure bursting/collapse/shrinkage may explain why expanded tofu exhibits higher deformation than Emmental cheese.

The expansion mechanism of Emmental cheese is rather special. Besides rheological properties of matrix and processing parameters, expansion is also controlled by free oil expulsion. The phenomena is rather complex because all these parameters are highly interdependent. The oil expulsion phenomena can be considered as the consequence of free oil formation that may be induced either by chemical transformation: extensive fat globule aggregation, coalescence and rupture during heating (Everett and Auty, 2008) or mechanical driving force (pressure). Some pools of remnant-free oil can fill the interstices of casein matrix. This free oil can enhance the meltability and in turn affect flowability and stretchability of molten cheese to expand during pressure drop.

Fat is known as glass transition depressor. Lowered quantity of free oil within the matrix, as consequence of the free oil expulsion, leads to higher glass transition temperature. This implies that the structure of molten cheese, in expanded state, is set sooner before the shrinkage occurred. Then the expansion is maximized and the shrinkage-deformation is minimized.

5. Conclusions

The instant controlled pressure drop (DIC) processing of protein-based foods (Emmental cheese and tofu) resulted in expanded and crispy snacks. These high-protein and poor-starch snacks can serve as an alternative for tasty and healthy snacks for the modern population. This new generation is more and more demanding healthy diet having 'clean label', i.e. passing less transformation and having minimum ingredients as possible.

The rapid camera enabled us to estimate the upper limit of time during which the volume expansion of materials occurs. It was impossible to observe continuously the dynamics of product puffing due to the creation of inherent mist. The shortest time of the mist presence was 64 ms. This time can be retained as the maximum time of the product volume expansion for all experiments.

Three expansion ratios were calculated using different measuring methods, i.e. sand pycnometry (r), direct dimension measurements by caliper (r_C) and dimension reading from camera images (r_I). The maximum of true expansion ratio of Emmental cheese ($r_{max} = 2.5$) was lower than the ratios $r_{C,max}$ (3.2) and $r_{I,max}$ (6). The differences among these values were partially explained by the shrinkage and deformation phenomena occurring during the pressure drop and post-drying. The lipid expulsion phenomenon during the pressure drop can favor expansion which depends among others on the quantity of remnant/endogenous/bound lipid.

The expansion ratios of tofu, $r_{C,\,max} = 4.2$ and $r_{I,\,max} = 10.5$, were higher than these of Emmental cheese. The differences in expansion level between these two foods can be explained by the difference in composition, rheological properties and glass transition temperature. Higher starch and lower lipid contents, and higher glass transition temperature can make tofu to be more expanded than Emmental cheese. The presence of fiber as ingredient can cause higher deformation of expanded tofu.

In the case of tofu, the differences in texture, generated by DIC are not due to changes in the composition as it is the case of Emmental cheese having high lipid content, which decreases in in function of DIC parameters.

Dairy and plant based protein foods underwent different expansion rate. Rheological behavior of the food matrices should be determined in function of thermo-mechanical treatment to get more insight into expansion mechanism.

Funding

This research did not receive any specific grant from funding agencies in the public, commercial, or not-for-profit sectors.

References

Agbisit, R., Alavi, S., Cheng, E., Herald, T.J., Trater, A.M., 2007. Relationships between microstructure and mechanical properties of cellular cornstarch extrudates. J. Texture Stud. 38, 199-219. https://doi.org/10.1111/j.1745-4603.2007.00094.x.

Allaf, K., Louka, N., Bouvier, J.M., Paren,t F., Forget, M., 1995. Methods for processing phytogenic materials to change their texture, apparatus therefor, and resulting materials, Patent WO9504466 (A1).

Allaf, T., and Allaf, K., 2014. Instant Controlled Pressure Drop (D.I.C.) in Food Processing from Fundamental to Industrial Applications. Springer Verlag, New York.

Albitar, N., Mounir, S., Besombes, C., Allaf, K., 2011. Improving the drying of onion using the instant controlled pressure drop technology. Drying Technol. 29, 993-1001. https://doi.org/10.1080/07373937.2010.507912.

Amon, M., Denson, C.D., 1984. A study of the dynamics of foam growth: Analysis of the growth of closely spaced spherical bubbles. Polym. Eng. Sci. 24, 1026–1034.

Arhaliass, A., Legrand, J., Vauchel, P., Pacha, F.F., Lamer, T., Bouvier, J. M., 2009. The effect of wheat and maize flours properties on the expansion mechanism during extrusion cooking. Food Bioprocess Technol. 2, 186 -193. https://doi.org/10.1007/s11947-007-0038-6

Arimi, J.M., Duggan, E., O'Sullivan, M., Lyng, J.G., O'Riordan, E.D., 2010. Effect of moisture content and water mobility on microwave expansion of imitation cheese. Food Chem. 121, 509-516. https://doi.org/10.1016/j.foodchem.2010.01.001.

Chanvrier, H., Chaunier, L., Della Valle, G., Lourdin, D., 2015. Flow and foam properties of extruded maize flour and its biopolymer blends expanded by microwave. Food Res. Int. 76, 567–575. https://doi.org/10.1016/j.foodres.2015.07.019.

Della Valle, G., Vergnes, B., Colonna, P., Patria, A., 1997. Relations between rheological properties of molten starches and their expansion behaviour in extrusion. J. Food Eng. 31, 277-295. http://dx.doi.org/10.1016/S0260-8774(96)00080-5.

Everett, D.W., Auty, M.A.E., 2008. Cheese structure and current methods of analysis. Int. Dairy J. 18, 759-773. https://doi.org/10.1016/j.idairyj.2008.03.012.

Gunasekaran, S., Mehmet, M.,Ak., 2002. Cheese Rheology and Texture, first ed. CRC Press.

Kristiawan, M., Sobolik, V., Allaf, K., 2008. Isolation of indonesian cananga oil by instantaneous controlled pressure drop. J. Essential Oil Res. 20, 135-146. https://doi.org/10.1080/10412905.2008.9699975.

Kristiawan, M., Sobolik, V., Al-Haddad, M., Allaf, K., 2008b. Effect of pressure-drop rate on the isolation of cananga oil using instantaneous controlled pressure-drop process. Chem. Eng. Proces. 47, 66–75.

Kristiawan, M, Chaunier, L., Della Valle, G., Ndiaye, A., Vergnes, B., 2016. Modeling of starchy melts expansion by extrusion. Trends Food Sci. Technol. 48, February 13-26. https://doi.org/10.1016/j.tifs.2015.11.004.

Logié N., Della Valle, G., Rolland-Sabaté, A., Descamps, N., Soulestin, J., 2018. How does temperature govern mechanisms of starch changes during extrusion? Carbohydr. Polym. 184, 57-65. https://doi.org/10.1016/j.carbpol.2017.12.040.

Louka, N., Allaf, K., 2004. Expansion ratio and color improvement of dried vegetables texturized by a new process "Controlled sudden decompression to the vacuum" Application to potatoes, carrot and onions, J. Food Eng. 65, 233-243. https://doi.org/10.1016/j.jfoodeng.2004.01.020.

Moraru, C.I., Kokini J.L., 2003. Nucleation and expansion during extrusion and microwave heating of cereal foods, Compr. Rev. Food Sci. Food Saf. 2, 147-165. https://doi.org/10.1111/j.1541-4337.2003.tb00020.x.

Mounir, S., Halle, D., Allaf, K., 2011. Characterization of pure cheese snacks and expanded granule powders textured by the instant controlled pressure drop (DIC) process. Dairy Sci. Technol. 91, 441. https://doi.org/10.1007/s13594-011-0023-8.

Ralet, M.C., Della Valle, G., Thibault, J.F., 1993. Raw and extruded fibre from pea hulls. Part I: Composition and physico-chemical properties. Carbohydr. Polym. 20, 17-23. https://doi.org/10.1016/0144-8617(93)90028-3.

Robin, F., Bovet, N., Pineau, N., Schuchmann, H.P., Palzer, S., 2011. Online shear viscosity measurement of starchy melts enriched in wheat bran. J. Food Sci. 76, E405-E412. https://doi.org/10.1111/j.1750-3841.2011.02193.x.

Robin, F., Dattinger, S., Boire, A., Forny, L., Horvat, M., Schuchmann, H. P., Palzer, S., 2012. Elastic properties of extruded starchy melts containing wheat bran using on-line rheology and dynamic mechanical thermal analysis. J. Food Eng. 109, 414–423. https://doi.org/10.1016/j.jfoodeng.2011.11.006.

Robin, F., Schuchmann, H.P., Palzer, S., 2012 b. Dietary fiber in extruded cereals: Limitations and opportunities. Trends Food Sci. Technol. 28, 23-32. https://doi.org/10.1016/j.tifs.2012.06.008.

Schwartzberg, H.G., WU, J.P.C., Nussinovitch, A., Mugerwa, J., 1995. Modelling Deformation and Flow During Vapor-induced Puffing, J. Food Eng. 25, 329-372. https://doi.org/10.1016/0260-8774(94)00015-2.

Singh, J., Singh, N., 1999. Effects of different ingredients and microwave power on popping characteristics of popcorn. J. Food Eng. 42, 161-165. https://doi.org/10.1016/s0260-8774(99)00114-4.

Stanley, W.D., 1989. Protein reactions during extrusion processing, in: Mercier, C., Linko, P., Harper, J.M. (Eds.), Extrusion cooking. American Association of Cereal Chemists, Inc., St. Paul, Minnesota, pp. 321-341.

Van der Sman, R.G.M., Broeze, J., 2014. Multiscale analysis of structure development in expanded starch snacks. J. Phys. Condensed Matter, 26, 464103. https://doi.org/10.1088/0953-8984/26/46/464103.

Van der Sman, R. G. M., (2016). Filler functionality in edible solid foams. Advances Colloid Interface Sci. 231, 23–35. https://doi.org/10.1016/j.cis.2016.03.003.

Verbeek, C.J.R., van den Berg, L.E., 2010. Extrusion processing and properties of protein-based thermoplastics. Macromol. Mater. Eng. 295, 10–21. https://doi.org/10.1002/mame.200900167.

Xu Y., Tao, Y., Shivkumar, S., 2016. Effect of freeze-thaw treatment on the structure and texture of soft and firm tofu. J. Food Eng. 190, 116-122. https://doi.org/10.1016/j.jfoodeng.2016.06.022.

Zotarelli, M.F., Porciuncula, B.D.A., Laurindo, J.B., 2012. A convective multi-flash drying process for producing dehydrated crispy fruits, J. Food Eng. 108, 523–531. https://doi.org/10.1016/j.jfoodeng.2011.09.014.

Media Video 1.avi

Graphical abstract

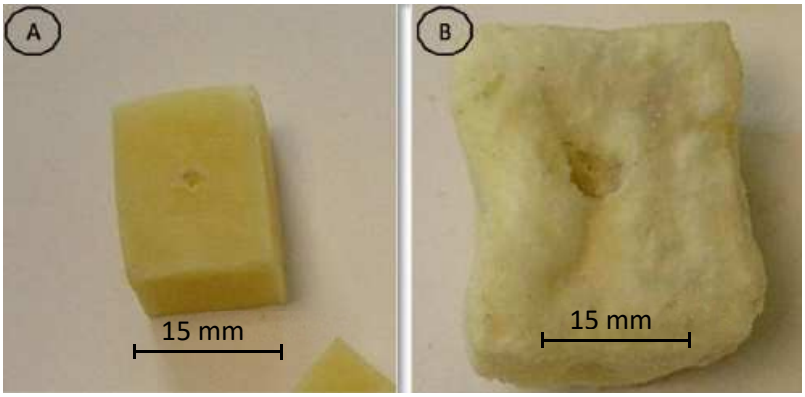

A) Emmental cheese before DIC treatment; B) expanded Emmental after treatment and post-drying.

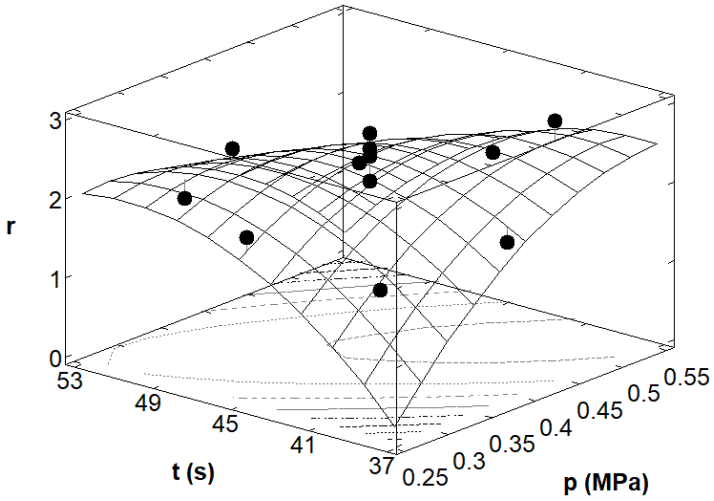

Effect of steam pressure *p* and treatment time *t* on expansion ratio *r* of Emmental cheese.